DNA damage checkpoint and recombinational repair differentially affect the replication stress tolerance of *smc6* mutants

Yu-Hung Chen[a,b,*], Barnabas Szakal[c], Federica Castellucci[c], Dana Branzei[c], and Xiaolan Zhao[a]
[a]Molecular Biology Program, Memorial Sloan-Kettering Cancer Center, New York, NY 10065; [b]Programs in Biochemistry, Cell, and Molecular Biology, Weill Graduate School of Medical Sciences of Cornell University, New York, NY 10021; [c]Institute of Molecular Oncology, Italian Foundation for Cancer Research, 20139 Milan, Italy

ABSTRACT **DNA damage checkpoint and recombinational repair are both important for cell survival of replication stress. Because these two processes influence each other, isolation of their respective contributions is challenging. Research in budding yeast shows that removal of the DNA helicase Mph1 improves survival of cells with defective Smc5/6 complex under replication stress. *mph1*Δ is known to reduce the levels of recombination intermediates in *smc6* mutants. Here, we show that *mph1*Δ also hyperactivates the Mec1 checkpoint. We dissect the effects of recombination regulation and checkpoint hyperactivation by altering the checkpoint circuitry to enhance checkpoint signaling without reducing recombination intermediate levels. We show that these approaches, similar to *mph1*Δ, lead to better survival of *smc6* cells upon transient replication stress, likely by ameliorating replication and chromosomal segregation defects. Unlike *mph1*Δ, however, they do not suppress *smc6* sensitivity to chronic stress. Conversely, reducing the checkpoint response does not impair survival of *smc6 mph1*Δ mutants under chronic stress. These results suggest a two-phase model in which *smc6* mutant survival upon transient replication stress can be improved by enhancing Mec1 checkpoint signaling, whereas *smc6* sensitivity to chronic stress can be overcome by reducing recombination intermediates.**

Monitoring Editor
Fred Chang
Columbia University

Received: Nov 27, 2012
Revised: May 29, 2013
Accepted: Jun 6, 2013

INTRODUCTION

Homologous recombination (HR) facilitates genome duplication under replication stress by repairing DNA strand breaks or single-strand DNA (ssDNA) gaps and restarting stalled replication forks (Aguilera and Gómez-González, 2008; Li and Heyer, 2008; Branzei and Foiani, 2010). During these processes, the strand exchange protein Rad51 coats ssDNA and enables ssDNA pairing with a homologous sequence to template new DNA synthesis. This leads to the formation of HR intermediates, such as D-loop and Holliday junction structures. A number of other proteins also play important roles in HR intermediate metabolism under these situations. In *Saccharomyces cerevisiae*, these include factors that promote HR intermediate formation or maintenance, such as the DNA helicase Mph1 and the Rad51 paralogue Shu complex (Mankouri *et al.*, 2007, 2009; Chen *et al.*, 2009; Choi *et al.*, 2010), and those that promote intermediate dissolution and resolution. The main dissolution factor is the STR complex, composed of the Sgs1 helicase, the topoisomerase Top3, and its partner, Rmi1 (Liberi *et al.*, 2005; Cejka and Kowalczykowski, 2010; Cejka *et al.*, 2010; Hickson and Mankouri, 2011). In addition, the octameric Smc5/6 complex, composed of Smc5, Smc6, and six other subunits (Nse1, Mms21, and Nse3–6; Zhao and Blobel, 2005; Kegel and Sjogren, 2010), also contributes to HR intermediate processing. The Smc5/6 complex is essential in budding yeast; like STR deletion mutants, its hypomorphic alleles show increased levels of HR intermediates that can be visualized as X-shaped structures (X-mols) on two-dimensional gel electrophoresis (2D gel; Zhao and Blobel, 2005; Branzei *et al.*, 2006; Chen *et al.*, 2009; Sollier *et al.*, 2009; Bermudez-Lopez *et al.*, 2010; Chavez *et al.*, 2010).

This article was published online ahead of print in MBoC in Press (http://www.molbiolcell.org/cgi/doi/10.1091/mbc.E12-11-0836) on June 19, 2013.

*Present address: Department of Biochemistry and Molecular Pharmacology, New York University School of Medicine, New York, NY 10016.

Address correspondence to: Xiaolan Zhao (zhaox1@mskcc.org).

Abbreviations used: FACS, fluorescence-activated cell sorting; HR, homologous recombination; MMS, methyl methanesulfonate; X-mol, X-shaped structure.

Although the aforementioned proteins have been primarily studied in the recombination context, they also affect other aspects of the replication stress response, particularly the DNA damage checkpoint. DNA structures generated during perturbed replication can be bound by checkpoint sensor proteins, such as the Rad17-Mec3-Ddc1 complex, referred to as 9-1-1 based on its homologues (RAD9-HUS1-RAD1). The 9-1-1 complex and other sensor proteins recruit and activate the apical checkpoint kinase Mec1 in budding yeast (Putnam *et al.*, 2009; Branzei and Foiani, 2010). Activated Mec1 in turn phosphorylates and activates the main effector kinase, Rad53. Further phosphorylation of a large number of substrates by Mec1 and Rad53 leads to changes promoting replication stress tolerance, such as replication fork stabilization, activation of DNA repair processes, and delayed cell cycle progression (Putnam *et al.*, 2009; Branzei and Foiani, 2010). Links between the DNA damage checkpoint and HR have been documented. Of most relevance is that proteins involved both in recombination intermediate formation and dissolution (or resolution) influence the DNA damage checkpoint but in an opposite manner. In budding yeast, *sgs1*Δ cells are defective in Rad53 activation (Frei and Gasser, 2000; Liberi *et al.*, 2005; Mankouri *et al.*, 2009), and in fission yeast, an *smc6* mutant fails to maintain the DNA damage checkpoint (Harvey *et al.*, 2004). In contrast, the lack of upstream HR factors, such as Rad51 and Shu, results in increased Rad53 activation, presumably due to increased ssDNA levels (Lee *et al.*, 2003; Mankouri *et al.*, 2007, 2009).

Because the foregoing mutants simultaneously affect HR and checkpoint, deconvoluting the mechanism underlying their genetic interactions is difficult. For example, removing Rad51 and the Shu complex improves the tolerance of *smc6* and *sgs1*Δ cells to replication stress (Shor *et al.*, 2005; Mankouri *et al.*, 2007; Ball *et al.*, 2009; Chen *et al.*, 2009; Choi *et al.*, 2010). This suppression could be interpreted as *rad51*Δ or *shu*Δ reducing levels of recombination intermediates or X-mols (Mankouri *et al.*, 2007; Chen *et al.*, 2009; Choi *et al.*, 2010). This interpretation would imply that X-mol accumulation is more toxic than the failure to initiate HR. However, because *rad51*Δ or *shu*Δ also increases the checkpoint response, the observed suppression could also be attributed to enhanced DNA damage checkpoint signaling. Thus far, it has been difficult to elucidate how recombination and DNA damage checkpoint separately affect the replication stress tolerance of *smc6* and *sgs1* mutants. Lack of this information prevents clear interpretation of the genetic observations and impedes our understanding of the physiological consequences of X-mol accumulation.

To address these issues, we examined a mutant allele of budding yeast Smc6, *smc6-P4*, which contains the K239R mutation. We previously showed that *smc6-P4* cells are extremely sensitive to replication stress and display an elevated level of X-mols when replicating in the presence of methyl methanesulfonate (MMS; Chen *et al.*, 2009). Both defects are suppressed by the removal of Mph1, Shu, or the proliferating cell nuclear antigen–polyubiquitinating enzyme Mms2, with *mph1*Δ having the strongest effect (Chen *et al.*, 2009; Choi *et al.*, 2010). Here we show that *smc6-P4* and *mph1*Δ exert opposite effects on the DNA damage checkpoint: *mph1*Δ increases it, whereas *smc6-P4* decreases it, and the *smc6-P4 mph1*Δ double mutant behaves like *mph1*Δ. To assess the contribution of increased checkpoint response to the replication stress tolerance of *smc6-P4*, we used two strategies that alter the checkpoint circuitry to enhance the DNA damage checkpoint. Both corrected Rad53 phosphorylation defects in *smc6-P4* cells without reducing X-mol levels. They also increased *smc6-P4* tolerance to transient, but not chronic, replication stress, whereas *mph1*Δ conferred tolerance to both. Furthermore, we reduced the checkpoint response in *smc6-P4 mph1*Δ double mutants by removing the checkpoint sensor protein Mec3 and found that *mph1*Δ can still suppress the sensitivity of *smc6-P4* cells to chronic replication stress. These results suggest that, whereas enhanced DNA damage checkpoint promotes tolerance to transient replication stress, X-mol removal is required for the survival of *smc6* mutants under persistent exposure to such stress.

RESULTS

smc6 and *mph1* mutations have opposite effects on the DNA damage checkpoint

The *mph1*Δ mutation strongly suppresses a number of *smc6*-mutant defects, notably conferring three orders of magnitude more resistance to the replication-blocking agent MMS (Chen *et al.*, 2009). Although our previously reported decrease in X-mol levels might be one cause (Chen *et al.*, 2009) of the strong suppression, additional mechanisms might also contribute. Because HR mutants influence the DNA damage checkpoint response, we examined whether *mph1*Δ and *smc6-P4* also alter this important replication stress tolerance mechanism and, if so, how this is related to the observed suppression.

We first examined how *mph1*Δ and *smc6-P4* affect Rad53 phosphorylation, a standard readout of the activation of Rad53 and DNA damage checkpoint. Rad53 phosphorylation is indicated by the appearance of a higher–molecular weight band on immunoblots and can be seen in wild-type cells after 0.03% MMS treatment (Figure 1A). After the same treatment, *mph1*Δ resulted in a complete upward shift of Rad53, a characteristic feature of Rad53 hyperphosphorylation (Figure 1A). In contrast, *smc6-P4* cells exhibited less Rad53 phosphorylation, as the phosphorylated Rad53 band (Rad53-P) is weaker in intensity than that of wild-type cells (Figure 1A). *smc6-P4 mph1*Δ double mutants behaved similarly to *mph1*Δ, indicating that *mph1*Δ results in Rad53 hyperphosphorylation in both wild-type and *smc6-P4* cells.

To determine whether the altered Rad53 phosphorylation levels in *smc6* and *mph1* mutants reflect a change in the initial activation or maintenance of Rad53 modification, we performed time course experiments in which G1-synchronized cells were released into MMS-containing media (Figure 1B). In wild-type cells, the Rad53-P band appeared at 20 min postrelease, peaked at 40 min, and diminished at 180 min, when most cells had finished replication, as judged by flow cytometry (fluorescence-activated cell sorting [FACS]; Figure 1, C and D). In *smc6-P4* cells, Rad53-P band was also visible 20 min postrelease, but the magnitude of phosphorylation did not reach the maximum level seen in wild-type (WT) cells (Figure 1C). This difference between the two strains could not be caused by cell-cycle progression changes, since their FACS profiles were similar (Figure 1D). We conclude that *smc6-P4* cells are defective in maximal Rad53 phosphorylation and, by extension, its activation.

In *mph1*Δ cells, Rad53 phosphorylation appeared to be stronger than wild type at 20 min and reached the maximum level at 40 min postrelease. Of importance, *mph1*Δ cells failed to attenuate Rad53 phosphorylation even at 180 min (Figure 1C). Consistent with persistent Rad53 phosphorylation, *mph1*Δ cells also exhibited a delay in S-phase progression compared with wild-type cells (Figure 1, C and D). *mph1*Δ *smc6-P4* cells behaved similarly to *mph1*Δ cells in terms of Rad53 phosphorylation level and S-phase progression (Figure 1, C and D). Therefore data from both asynchronous and time course experiments show that *smc6-P4* and *mph1*Δ have opposite effects on Rad53 phosphorylation and that *mph1*Δ is epistatic to *smc6-P4* for this phenotype.

Because mutations of key residues in the Mph1 helicase domain (*mph1-hd*) that abolish its helicase activity suppress *smc6-P4*'s MMS

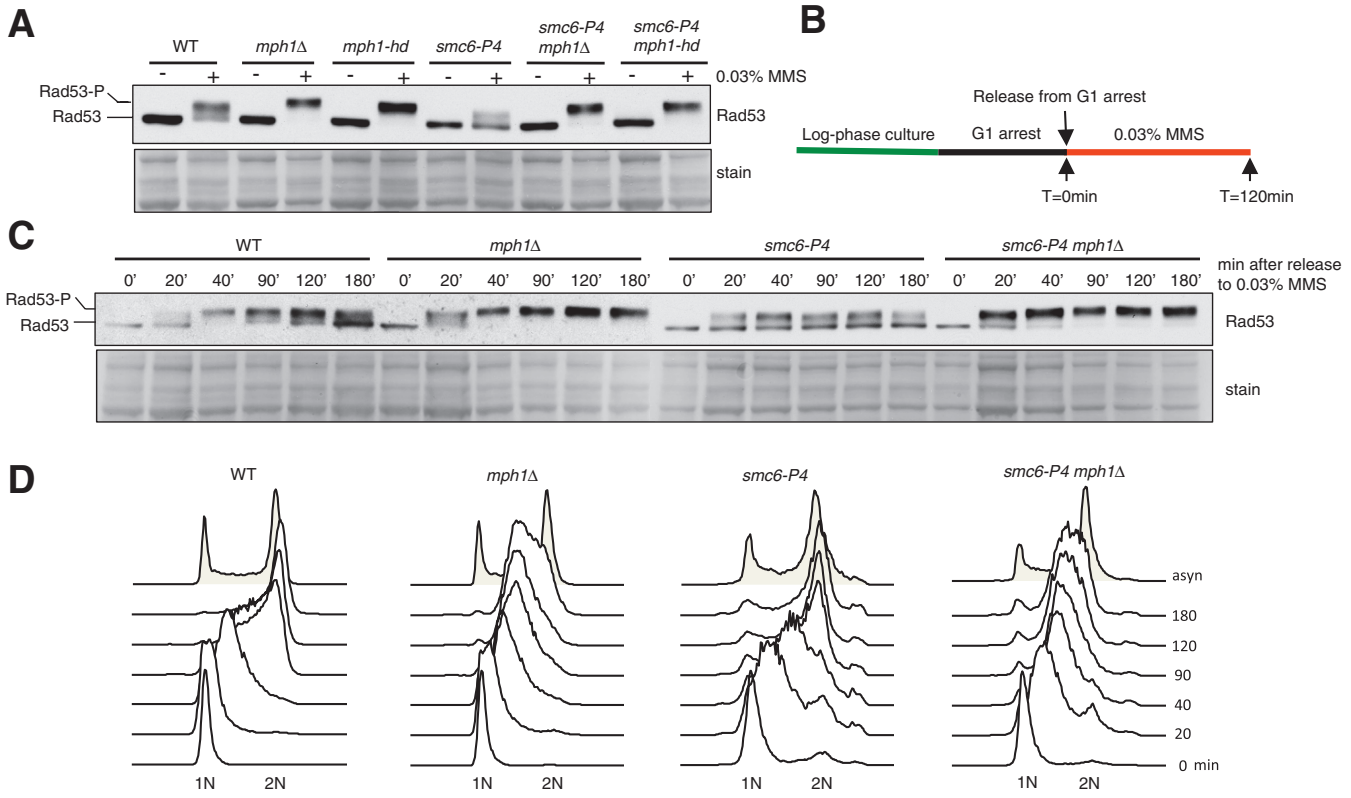

FIGURE 1: Examination of Rad53 phosphorylation and bulk replication in cells defective in Mph1 and Smc6. (A) *mph1* and *smc6* mutations differentially affect Rad53 activation. Exponentially growing asynchronous cultures were treated with 0.03% MMS for 2 h. Rad53 phosphorylation was examined in cells before (–) and after (+) MMS treatment by Western blot. The levels of Rad53 phosphorylation were decreased in *smc6-P4* but increased in *mph1*Δ, *mph1-hd*, *smc6-P4 mph1*Δ, and *smc6-P4 mph1-hd* cells. Bottom, amido black stain of the gel. The bands representing unmodified and phosphorylated Rad53 are labeled as Rad53 and Rad53-P, respectively. (B–D) Examination of the kinetics of Rad53 phosphorylation in *mph1*Δ, *smc6-P4*, and *mph1*Δ *smc6-P4* cells. (B) Schematic of the experimental procedure. G1-synchronized cells were released into media containing 0.03% MMS. Cells were withdrawn at the indicated time points to monitor Rad53 phosphorylation by Western blot and DNA contents by FACS. (C) On treatment with MMS, *smc6-P4* cells show reduced Rad53 phosphorylation, whereas *mph1*Δ and *smc6-P4 mph1*Δ cells exhibit persistent Rad53 phosphorylation. (D) *mph1*Δ and *mph1*Δ *smc6-P4* cells display slower S-phase progression in MMS-containing media than WT and *smc6-P4* cells. FACS analysis of samples from C are shown with those of asynchronous cultures (asyn).

sensitivity and X-mol accumulation similarly to *mph1*Δ (Chen *et al.*, 2009), we asked whether *mph1-hd* also affects the DNA damage checkpoint. We found that *mph1-hd* behavior resembled that of *mph1*Δ in both asynchronous and synchronized experiments. *mph1-hd* cells showed Rad53 hyperphosphorylation and slower S-phase progression, regardless of Smc6 status (Figure 1A and Supplemental Figure S1). Thus the lack of Mph1 helicase activity accounts for the observed effects on the DNA damage checkpoint. These results raise the possibility that the mounting of a more robust DNA damage checkpoint response is partly responsible for *mph1* suppression of *smc6-P4* MMS sensitivity. This effect could serve to stabilize stalled replication forks and provide more time for repairing DNA lesions.

Mec1 is required for the persistence of Rad53 phosphorylation and slow S-phase progression in *mph1*Δ mutants

In budding yeast, Mec1 is the main checkpoint kinase that controls Rad53 activation and S-phase progression, and its homologue, Tel1, makes minor contributions (Putnam *et al.*, 2009; Branzei and Foiani, 2010). To assess whether the observed *mph1* effect on the DNA damage checkpoint is due to a change in the Mec1-dependent pathway, we examined *mec1*Δ cells containing *sml1*Δ, a suppressor of *mec1*Δ lethality that does not affect checkpoint function (Zhao *et al.*, 1998). As shown in Figure 2A and consistent with the literature, *mec1*Δ cells contain unphosphorylated Rad53 and progress through S phase more rapidly than wild-type cells after MMS treatment. The removal of Mec1 in *mph1*Δ or *mph1*Δ *smc6-P4* cells largely abolished Rad53 phosphorylation and the observed S-phase delay (Figures 2, A and B). We conclude that the increased Rad53 phosphorylation and delayed replication seen in both *mph1*Δ and *mph1*Δ *smc6-P4* cells are dependent on Mec1-mediated checkpoint activities. Delayed replication in wild-type cells under genotoxic stress is due to Mec1-mediated inhibition of late replication origin firing (Santocanale and Diffley, 1998; Shirahige *et al.*, 1998). Thus this is more likely accountable for the S-phase delay in *mph1* mutants than an inability to repair damaged DNA.

TEL1-hy909 promotes the survival of *smc6-P4* cells upon transient, but not chronic, replication stress

Because *smc6-P4 mph1*Δ cells exhibit higher Rad53 phosphorylation levels than *smc6-P4* cells, we asked whether enhancing the DNA damage checkpoint alone could improve the replication stress tolerance of *smc6-P4* cells. To this end, we used two different

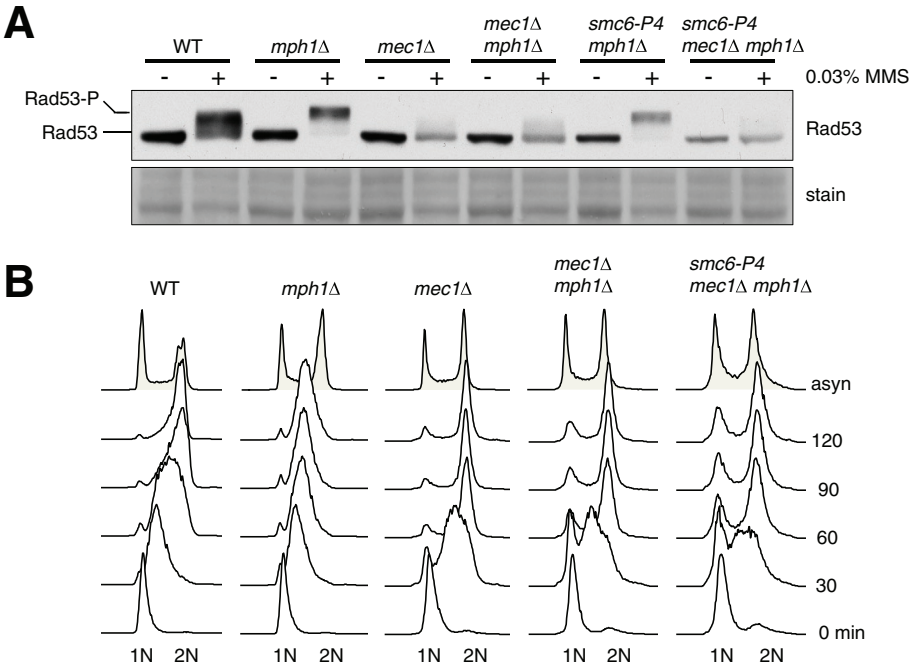

FIGURE 2: Mec1-mediated Rad53 hyperphosphorylation and slower DNA synthesis in cells containing *mph1*Δ. (A) *mec1*Δ abolishes Rad53 hyperphosphorylation in *mph1*Δ and *mph1*Δ *smc6-P4* cells. Rad53 phosphorylation was analyzed in asynchronous cells as described in Figure 1A. (B) *mec1*Δ reverts the slow S-phase progression in *mph1*Δ and *mph1*Δ *smc6-P4* cells. Cells were synchronized and released as in Figure 1B, and DNA content was monitored by FACS. All *mec1*Δ cells contain the lethality suppressor *sml1*Δ.

approaches that directly alter checkpoint circuitry. The first approach used the *TEL1-hy909* gain-of-function allele, which results in elevated Tel1 kinase activity and Rad53 hyperphosphorylation (Baldo *et al.*, 2008). We confirmed Rad53 hyperphosphorylation in *TEL1-hy909* cells after MMS treatment in a time course experiment (Supplemental Figure S2A). The degree of Rad53 hyperphosphorylation caused by *TEL1-hy909* is similar to that seen with *mph1*Δ, although only the latter slows S-phase progression (Supplemental Figure S2A). As reported previously, *TEL1-hy909* greatly improved the survival of *mec1*Δ cells during chronic exposure to MMS (Supplemental Figure S2A; Baldo *et al.*, 2008). These results together indicate that *TEL1-hy909* augments a critical aspect of the Mec1-mediated checkpoint response to increase viability in MMS-containing media. That *TEL1-hy909* did not significantly affect late replication origin firing as reflected by FACS analysis is consistent with the notion that this aspect of checkpoint control is not essential for cell survival upon replication stress (Tercero *et al.*, 2003).

After confirming that *TEL1-hy909* can hyperactivate checkpoint under our experimental conditions, we examined its effect on the checkpoint response, recombination intermediate levels, and MMS sensitivity of *smc6-P4* cells in a time course experiment. First, we found that *TEL1-hy909* increased the level of Rad53 phosphorylation in *smc6-P4* cells, albeit less strongly than *mph1*Δ (Figure 3A). *TEL1-hy909* did not affect S-phase progression as seen in wild-type cells (Figure 3A). Consistent with its observed Rad53 hyperphosphorylation and like *mph1*Δ, *TEL1-hy909* resulted in a greater degree of degradation of the ribonucleotide reductase inhibitor Sml1, another frequently used readout of DNA damage checkpoint function (Figure 3A and Supplemental Figure S3A; Zhao *et al.*, 2001). Second, *TEL1-hy909* did not reduce X-mol levels in *smc6-P4* cells throughout the time course, suggesting that increased checkpoint response does not grossly decrease HR intermediate levels (Figure 3B). Third, *TEL1-hy909* improved the viability of *smc6-P4* cells to a similar degree as *mph1*Δ when cells were withdrawn at each time point to assess survival (Figure 3C). Thus hyperactivation of the DNA damage checkpoint alone without reducing X-mol levels is sufficient for improving the tolerance of *smc6-P4* cells to transient replication stress.

Next we examined how *TEL1-hy909* affects *smc6-P4* cell survival during chronic MMS exposure. We found that, unlike *mph1*Δ, *TEL1-hy909* did not improve the viability of *smc6-P4* cells during chronic exposure to MMS, even at a concentration lower than the one at which it suppresses the lethality of *mec1*Δ (Figure 3D). Taken together, the results indicate that increasing Rad53 phosphorylation levels by *TEL1-hy909* promotes the survival of *smc6-P4* cells after transient but not chronic exposure to MMS.

TEL1-hy909 improves chromosomal replication and segregation of *smc6-P4* cells

To understand how DNA damage checkpoint hyperactivation improves *smc6-P4* tolerance to transient replication stress, we examined both chromosomal replication and segregation. Because *smc6-P4* cells began to lose viability in S phase when treated with MMS, we first examined chromosomal replication using pulsed-field gel electrophoresis (PFGE). We treated G1 cells with a pulse of MMS and then released them into the cell cycle in normal media (Figure 4A). Based on the criterion that only fully replicated chromosomes can enter the gel, wild-type cells appeared to complete replication at around 60 min (Figure 4, A–C). In contrast, *smc6-P4* cells failed to finish chromosomal replication even at 240 min postrelease. Introduction of *TEL1-hy909* increased extent of replication completion in *smc6-P4* cells (Figure 4, A–C). These results suggest that enhanced checkpoint response can improve replication capacity in *smc6-P4* cells after transient MMS treatment.

We also assessed chromosome segregation at 240 min postrelease in the foregoing experiment. Compared with wild type, *smc6-P4* strains exhibited fewer normal anaphase and telophase cells but more large-budded cells with missegregated or mispositioned nuclei ($p < 0.05$; Figure 4, D and E). *TEL1-hy909* increased the former populations and decreased the latter ($p < 0.05$; Figure 4, D and E). One interpretation is that correction of checkpoint defect in *smc6-P4* cells by *TEL1-hy909* is sufficient to improve chromosome segregation, leading to better survival.

Induced proximity of Ddc1 and Ddc2 enhances DNA damage checkpoint response and improves survival of *smc6-P4* cells upon transient exposure to MMS

We also used another strategy to increase checkpoint response, on the basis of the observation that induced proximity of the DNA damage checkpoint sensor protein Ddc1 and the Mec1 binding partner Ddc2 is sufficient to activate checkpoint (Bonilla *et al.*, 2008). In this system, Ddc1 and Ddc2 are fused to LacI–green fluorescent

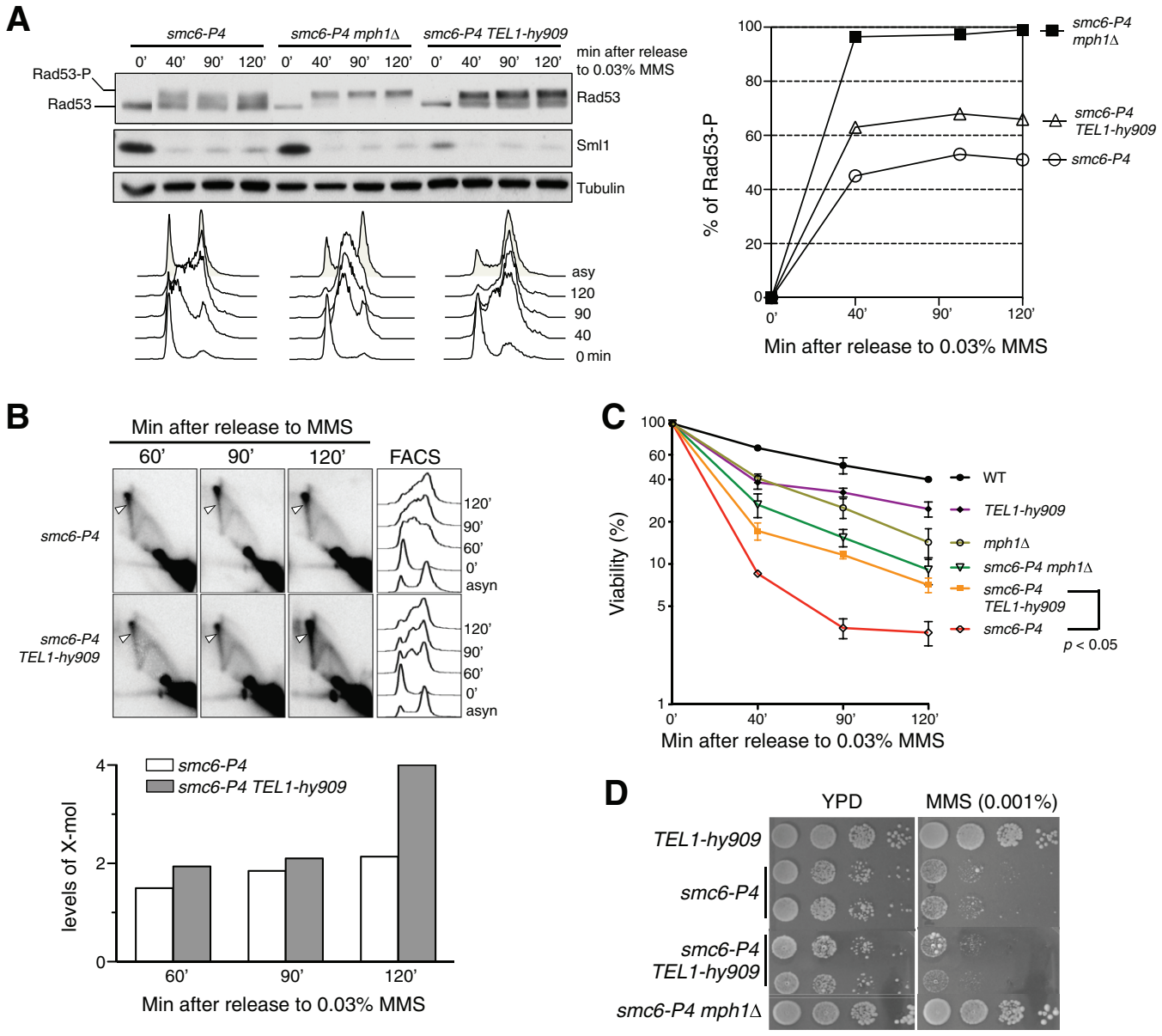

FIGURE 3: The effects of *TEL1-hy909* on the DNA damage checkpoint and MMS sensitivity of *smc6-P4* cells. (A) *TEL1-hy909* increases Rad53 phosphorylation and Sml1 degradation in *smc6-P4* cells. Experiments were carried out as described in Figure 1B. *TEL1-hy909* increases Rad53 phosphorylation in *smc6-P4* as shown by Western blot (left) and quantification (right). The level of Sml1 protein was examined (middle) and quantified using tubulin as a loading control in Supplemental Figure S3A. FACS analysis for each strain is shown below the blot. (B) *TEL1-hy909* does not affect X-mol levels in *smc6-P4* cells. Cells were treated as in A. Recombination intermediates, that is, X-mols (arrowheads) at the ARS305 region were analyzed by 2D gel electrophoresis at indicated time points. Right, FACS profiles. Bottom, quantification of X-mol levels. (C) *TEL1-hy909* improves survival of *smc6-P4* cells after transient exposure to MMS. Experiments were carried out as in A. Cells of indicated genotypes were plated out to determine the survival percentage of colonies at indicated time points. Each time point represents the mean of two independent experiments, and the SD is given. *p* value denotes that the difference in the viability of *smc6-P4* and *smc6-P4 TEL1-hy909* cells is statistically significant. (D) *TEL1-hy909*, unlike *mph1*Δ, does not suppress the sensitivity of *smc6-P4* to chronic exposure to MMS.

protein (GFP) modules, and their targeting to chromosomal LacO arrays results in Rad53 phosphorylation and checkpoint activation even without DNA damage in S and G2/M phases. This likely occurs via Mec1-Ddc2 recruitment to chromatin by the 9-1-1 complex (Bonilla *et al.*, 2008). We tested how this system affects DNA damage checkpoint responses, X-mol levels, and replication stress tolerance in *smc6-P4* cells.

The expression of Ddc1 and Ddc2 fusion constructs was induced by a pulse of galactose in G1-arrested cells before the cells were released into MMS-containing glucose media. Because this system activates Rad53 even without DNA-damaging agents, we used a lower concentration of MMS (0.005%). Time course experiments show that this induction led to Rad53 hyperphosphorylation in both WT and *smc6-P4* backgrounds (Figure 5A; compare the lanes with

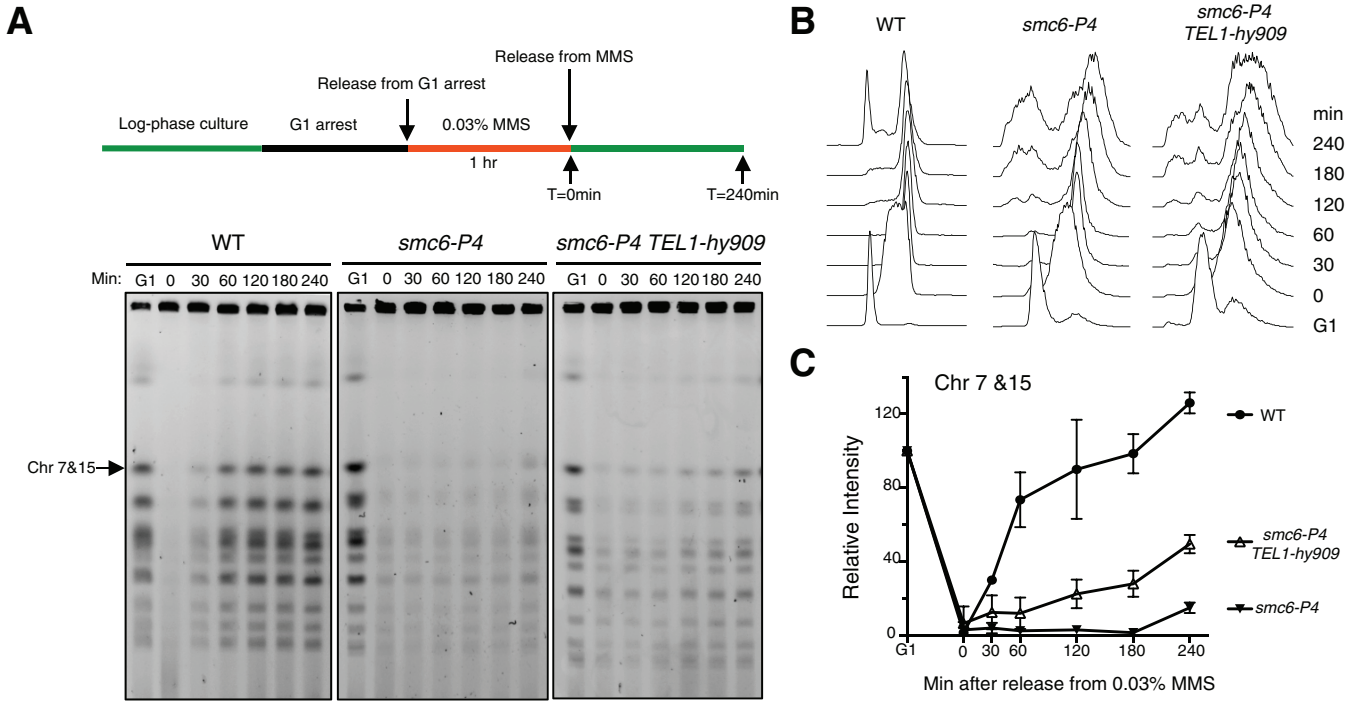

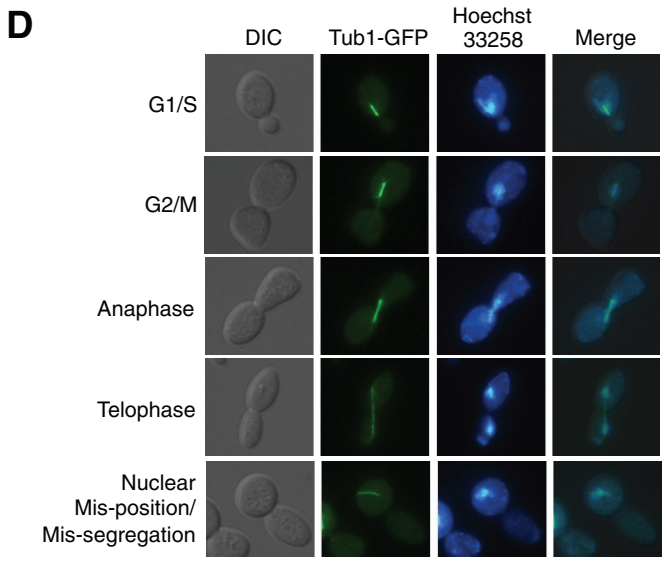

	WT (n=207/186)	*smc6-P4* (n=143/150)	*smc6-P4 TEL1-hy909* (n=141/140)
G1/S	43.6%	32.5%	31.3%
G2/M	26.3%	31.4%	31.0%
Anaphase	7.9%	3.1% (p<0.05)	17.4% (p<0.05)
Telophase	14.1%	3.8% (p<0.05)	8.2% (p<0.05)
Nuclear Mis-position/ Mis-segregation	3.2%	25.9% (p<0.05)	8.6% (p<0.05)

FIGURE 4: *TEL1-hy909* improves chromosome replication and segregation in *smc6-P4* cells. (A–C) Pulsed field gel electrophoresis analysis of cells with the indicated genotype during the course of recovery from transient MMS treatment (A). (A, top) Experimental scheme. (B) FACS analysis of the examples. (C) Quantification of representative chromosomal bands. The relative intensity of the chromosomal bands in *smc6-P4* and *smc6-P4 TEL1-hy909* at 180 and 240 min postrelease are statistically different ($p < 0.05$, Student's *t* test). Standard deviations for each time point are depicted. (D) Examination of nuclear segregation. Cells were treated as in A–C and microscopically examined at 240 min postrelease. Left, representative pictures of each category of cells, with Tub1-GFP marking the spindle and Hoechst staining of the nucleus. Cells were categorized as previously described (Tanaka *et al.*, 2005). Briefly, G1/S cells have no or small buds with single nucleus and short spindle in the mother cells; G2/M cells have medium to large buds with single nucleus close to the bud neck and a short spindle; anaphase cells have large buds with nucleus spanning between two cells and medium-length spindle; telophase cells have large buds with separated nuclei and elongated spindle; large-budded cells with nucleus away from the bud neck were categorized as nuclear mispositioning or missegregation. Two independent spores were examined for each genotype, and cell number (*n*) is indicated. The average percentage of each category of cells is shown. Statistically significant differences between WT and *smc-6-P4* and between *smc6-P4* and *smc6-P4 TEL1-hy909* are denoted below *smc6-P4* and *smc6-P4 TEL1-hy909*, respectively.

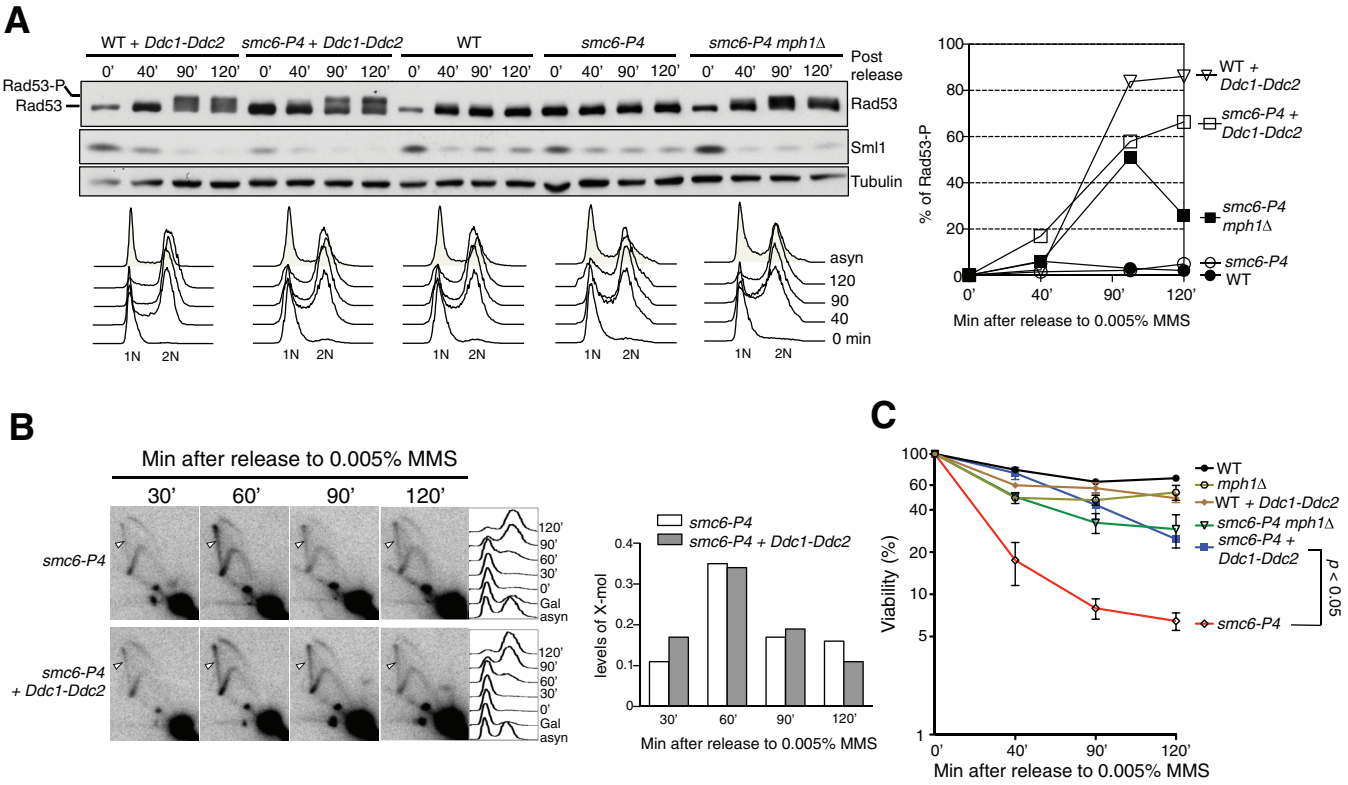

FIGURE 5: Juxtaposition of Ddc1 and Ddc2 increases DNA damage checkpoint response and improves tolerance to acute treatment of MMS in *smc6-P4* cells. (A) Induction of the Ddc1 and Ddc2 fusion constructs (Ddc1-Ddc2) increases Rad53 phosphorylation and Sml1 degradation in both wild-type and *smc6-P4* cells. G1-arrested cells were induced for the expression of this system and released into MMS-containing media. Protein samples and DNA content were examined as in Figure 3A. (B, C) Induction of the Ddc1 and Ddc2 juxtaposition does not reduce X-mol levels but improves *smc6-P4* cell survival upon transient exposure to MMS. The 2D gel analysis of X-mols (arrowheads, B) and viability test (C) were performed as in Figure 3. The *p* value denotes that the difference in the viability of indicated strains is statistically significant.

and without expression of the constructs). This effect on Rad53 phosphorylation is similar to that induced by *mph1*Δ (Figure 5A). Consistent with this, lower levels of the Sml1 protein were detected when Ddc1 and Ddc2 fusions were induced in both WT and *smc6-P4* cells (Figure 5A and Supplemental Figure S3B). Examination of replication intermediates by 2D gel found that the engineered Ddc1-Ddc2 juxtaposition did not alter X-mol levels in *smc6-P4* cells (Figure 5B). Finally, this system was as effective as *mph1*Δ in improving *smc6-P4* survival after transient exposure to MMS (Figure 5B). These results are consistent with those obtained for *TEL1-hy909;* taken together, they strongly suggest that increasing Rad53 activation in *smc6-P4* cells is sufficient for increasing their resistance to transient replication stress. Because prolonged expression of the Ddc1 and Ddc2 fusions can impair replication (Bonilla *et al.*, 2008), this system cannot be used to evaluate responses to chronic MMS exposure.

Removal of DNA damage checkpoint sensor proteins Mec3 and Rad24 does not affect *smc6-P4 mph1*Δ tolerance of chronic MMS treatment

The results obtained so far suggest that correcting Rad53 phosphorylation in *smc6-P4* cells by *TEL1-hy909* or the juxtaposition of Ddc1 and Ddc2 can increase cellular tolerance to transient but not chronic MMS exposure. To determine directly whether *mph1*Δ-mediated checkpoint hyperactivation contributes to the viability of *smc6-P4 mph1*Δ cells upon chronic MMS treatment, we reduced the checkpoint response in this double mutant by removing the checkpoint sensor protein Mec3.

Unlike *mec1*Δ, which exhibited strong synthetic sickness with *mph1*Δ in the presence of MMS (Supplemental Figure S2C), *mec3*Δ did not appear to affect *mph1*Δ survival on MMS-containing media (Supplemental Figure S4). Thus it is possible to determine whether reducing checkpoint response via *mec3*Δ affects the suppression of *smc6-P4* cells by *mph1*Δ. As shown in Figure 6A, *mec3*Δ diminished Rad53 phosphorylation in *mph1*Δ, *smc6-P4*, and *smc6-P4 mph1*Δ cells. Quantification showed that *mec3*Δ effectively reduced Rad53 phosphorylation levels in *smc6-P4 mph1*Δ cells such that the triple mutant displays a similar degree of Rad53 phosphorylation as *smc6-P4* cells (Figure 6B). Of importance, *mec3*Δ did not alter X-mol levels significantly in either *smc6-P4* or *smc6-P4 mph1*Δ cells in time course experiments when G1 cells were released into MMS-containing media (Figure 6C). Finally, we found that *mph1*Δ still conferred robust suppression of *smc6-P4* MMS sensitivity in the absence of Mec3 (Figure 6D). A similar effect was also seen with removal of the Mec3 loader, Rad24 (Figure 6D and Supplemental Figure S4). Taken together, these results suggest that improvement of *smc6-P4* survival of chronic MMS exposure by *mph1*Δ is more a consequence of reduced X-mol levels than of enhanced checkpoint response.

DISCUSSION

Unraveling the genetic relationships between some recombinational repair proteins is complicated by their additional effects on the DNA

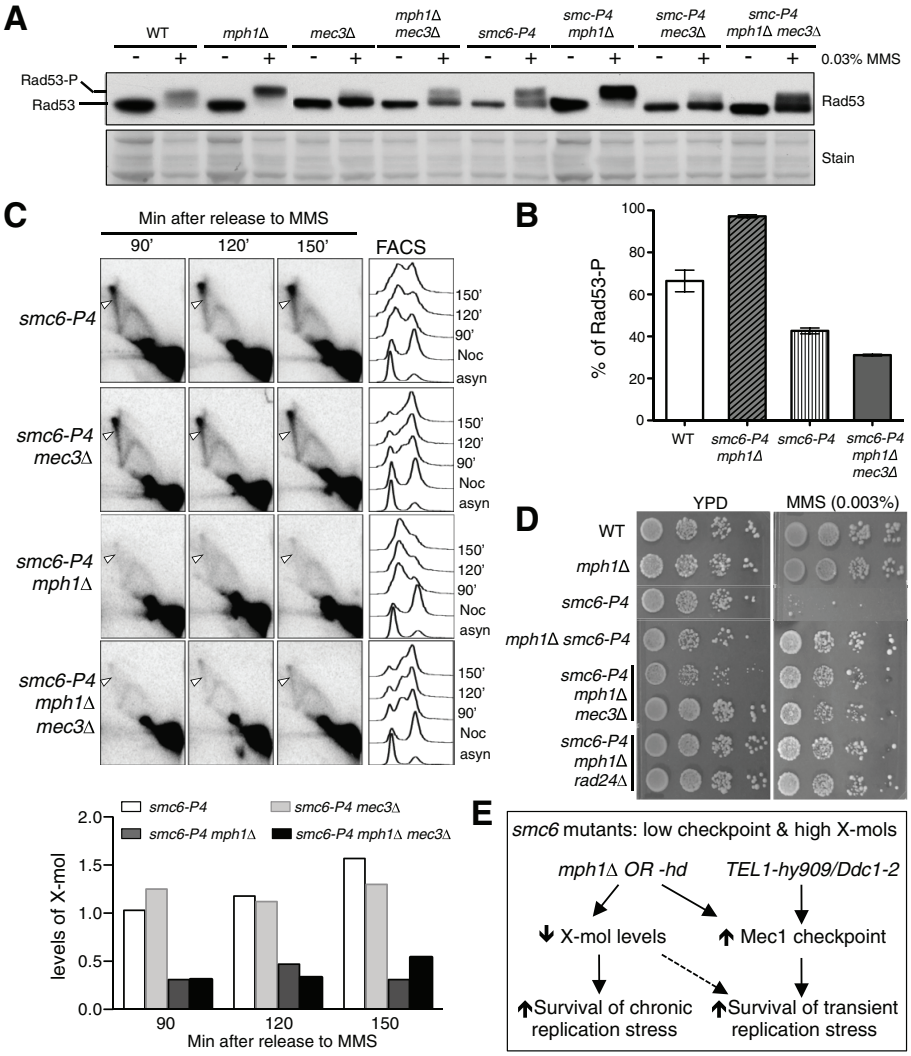

FIGURE 6: *mec3*Δ reduces Rad53 phosphorylation without affecting X-mol levels or survival upon MMS treatment in *smc6-P4* and *smc6-P4 mph1*Δ cells. (A, B) *mec3*Δ decreases Rad53 phosphorylation upon MMS treatment. Cells were treated as in Figure 1, and Rad53 phosphorylation is examined in A and quantified in B. The percentage of Rad53-P in *smc6-P4 mph1*Δ *mec3*Δ is statistically different from that in *smc6-P4* and *smc6-P4 mph1*Δ cells ($p < 0.05$, Student's *t* test). (C) Removal of Mec3 does not affect X-mol levels in *smc6-P4* or *smc6-P4 mph1*Δ cells. Experiments were carried out as in Figure 3B. (D) Neither *mec3*Δ nor *rad24*Δ affects *mph1*Δ suppression of *smc6-P4* sensitivity upon chronic exposure to MMS. (E) A summary of the results and a model for the differential effects of checkpoint and recombination on *smc6* mutant tolerance to replication stress. More details are given in the *Discussion*.

damage checkpoint. We previously showed that removing the DNA helicase Mph1 or mutating its key enzymatic residues reduces X-mol levels and strongly suppresses the MMS sensitivity of *smc6-P4* cells (Chen *et al.*, 2009). Our new data show that *smc6-P4* and *mph1*Δ (or *mph1-hd*) have opposing effects on the Mec1 checkpoint. *smc6-P4* cells failed to phosphorylate Rad53 to wild-type levels upon MMS treatment, whereas *mph1*Δ (or *mph1-hd*) exhibited persistent Rad53 phosphorylation (Figure 1 and Supplemental Figure S1). Although the underlying reason for these effects is not entirely clear, it likely pertains to alteration of ssDNA levels or replisome stability as suggested for similar situations (Cobb *et al.*, 2005, Harvey *et al.*, 2004; Alabert *et al.*, 2009; Yeung *et al.*, 2011). Besides Rad53 hyperphosphorylation, *mph1*Δ (or *mph1-hd*) also resulted in a strong Mec1-dependent S-phase delay, and *smc6-P4 mph1*Δ behaved like *mph1*Δ (Figure 2). These novel observations of DNA damage checkpoint effects raised the question of whether an enhanced checkpoint response is sufficient to improve *smc6-P4* survival upon replication stress.

To address this question, we used two different approaches to augment the DNA damage checkpoint response without affecting X-mol levels. Both the hyperactive *TEL1-hy909* allele and the induced proximity of Ddc1 and Ddc2 increased Rad53 phosphorylation levels in cells with normal and defective Smc6 upon MMS treatment, with a stronger effect seen in the latter (Figures 3A and 5A and Supplemental Figure S2A). Both resulted in a greater degree of Sml1 degradation, consistent with an enhanced checkpoint response (Figures 3A and 5A and Supplemental Figure S3). Neither *TEL1-hy909* nor the Ddc1-Ddc2 system lowered the level of X-mols in *smc6-P4* cells, suggesting that checkpoint hyperactivation does not affect HR intermediate levels and that these alleles can be used to isolate checkpoint- from HR-dependent effects (Figures 3B and 5B). We found that both strategies improved the replication stress tolerance of *smc6-P4* cells during a time course of 2-h exposure to MMS (Figures 3C and 5C). We note that *TEL1-hy909* also improved the checkpoint response and survival of another *smc6* mutant, *smc6-56*, after exposure to transient replication stress (Supplemental Figure S5, A and B). Thus improved *smc6* mutant resistance to acute replication stress can be achieved solely by DNA damage checkpoint hyperactivation. Our results further show that an enhanced checkpoint response can improve replication capacity and chromosomal segregation in *smc6-P4* cells (Figure 4, A–D). This is presumably achieved by promoting replication fork stability and allowing more time for nuclear segregation. However, other effects, such as those involving previously reported effects on kinetochore and spindle functions (Yong-Gonzales *et al.*, 2012), may also contribute.

Although *TEL1-hy909* suppressed *smc6-P4* sensitivity during transient MMS exposure to a similar extent as *mph1*Δ, only *mph1*Δ promoted the survival of *smc6-P4* cells during chronic MMS treatment (Figure 3D). This argues that the observed suppression by *mph1*Δ involves more than just checkpoint hyperactivation. This idea is further supported by the observation that *mph1*Δ still confers suppression to *smc6-P4* cells under chronic and transient MMS treatment upon *MEC3* deletion, which reduced the checkpoint response without affecting X-mol level (Figure 6, A–D, and data not shown). Thus the observed *mph1* suppression is at least partly due to a reduction in recombination intermediate levels. We note that a recent study reports the ability of *mec3*Δ to partially reduce X-mol levels in *sgs1*Δ cells (Karras *et al.*, 2013), whereas we detected no such effect in *smc6-P4* cells (Figure 6C). This difference is consistent

with previously noted differences in the effect of *mph1*Δ on X-mol levels in *smc6-P4* versus *sgs1*Δ cells (Chen *et al.*, 2009; Mankouri *et al.*, 2009), thus arguing for differential pathway involvement of the Smc5/6 complex versus Sgs1, in addition to their common functions.

On the basis of our results, we propose a two-phase model to explain the severe sensitivity of *smc6* mutant cells to replication stress (Figure 6E). When replication forks are stalled due to transient stress, a strong DNA damage checkpoint response is advantageous to *smc6* mutants. On chronic exposure to replication stress, however, preventing HR intermediate accumulation becomes the dominant factor for mutant cell survival. In this model, the checkpoint-related and X-mol regulation functions of the Smc5/6 complex are separable. This model may also be applicable to other mutants, such as *sgs1*Δ and *esc2*Δ, as they also exhibit X-mol accumulation and checkpoint defects and their MMS sensitivity is suppressed by the removal of recombination factors such as Rad51 and Shu (Liberi *et al.*, 2005; Mankouri *et al.*, 2009; Sollier *et al.*, 2009; Choi *et al.*, 2010). The tools used here to dissect the contributions of checkpoint hyperactivation and recombination may be useful for evaluating these cases as well. Our observation that neither hyperactivation nor reduction of checkpoint in *smc6-P4* cells affected HR intermediate levels suggests that checkpoint does not affect at least one branch of recombination-mediated damage bypass. This extends previous observations that checkpoint does not inhibit all modes of recombinational repair under replication stress, although it hinders those at chromosomal breaks, as measured by Rad52 foci levels (Lisby *et al.*, 2004; Alabert *et al.*, 2009; Barlow and Rothstein, 2009). In addition, our findings may be related to those in higher eukaryotes, in which the regulation of HR products is important for prolonged but not transient exposure to replication stress (Petermann *et al.*, 2010). Compounded, these studies begin to unravel the complex interplay between checkpoint and recombinational repair. Further investigation into the underlying mechanisms of this interplay will provide insight into how these two important genotoxic tolerance mechanisms are coordinated at the molecular level.

MATERIALS AND METHODS

Yeast strains

The yeast strains used in this study are listed in Table 1 and Supplemental Table 1. They are derivatives of W1588-4C, a *RAD5* derivative of W303 (*MAT***a** *ade2-1 can1-100 ura3-1 his3-11,15 leu2-3112 trp1-1 rad5-535*; Thomas and Rothstein, 1989). Only one strain for each genotype is listed, but at least two independent spore clones of each genotype were used in each of the experiments. Standard yeast protocols were used for strain construction, growth, and medium preparation. The construction of *smc6-P4* and *smc6-56* strains was described previously (Chen *et al.*, 2009).

Name	Relevant genotype
X3117-8B	*MATa RAD53-3Flag::LEU2*
X3117-16B	*MATa RAD53-3Flag::LEU2 mph1Δ::KAN*
X3223-19A	*MATa RAD53-3Flag::LEU2 smc6-P4-13Myc::HIS3*
X3117-15A	*MATa RAD53-3Flag::LEU2 smc6-P4-13Myc::HIS3 mph1Δ::KAN*
X3660-8C	*MATa RAD53-3Flag::LEU2 mph1-Q603D::HIS3*
X3660-5C	*MATa RAD53-3Flag::LEU2 smc6-P4-13Myc::KAN mph1-Q603D ::HIS3*
X3659-18D	*MATa RAD53-3Flag::LEU2 mec1Δ::TRP1 sml1Δ::HIS3*
X3659-14D	*MATa RAD53-3Flag::LEU2 mec1Δ::TRP1 sml1Δ::HIS3 mph1Δ::KAN*
X3659-12C	*MATa RAD53-3Flag::LEU2 mec1Δ::TRP1 sml1Δ::HIS3 smc6-P4-13Myc::KAN mph1Δ::KAN*
X3445-5A	*MATa RAD53-3Flag::LEU2 smc6-P4-13myc::HIS3 TEL1-hy909 ::LEU2*
X3845-7B	*MATa RAD53-HA::LEU2 GalS-DDC1-GFP-LacI::URA3 Gal-DDC2-GFP-LacI::HIS3 ddc1Δ LacO::TRP1*
X3845-11C	*MATa smc6-P4-13myc::KAN RAD53-HA::LEU2 GalS-DDC1-GFPLacI::URA3 Gal-DDC2-GFP-LacI::HIS3 LacO::TRP1*
X4186-5D	*MATa RAD53-3Flag::LEU2 mec3Δ::URA3*
X4186-6D	*MATa RAD53-3Flag::LEU2 mec3Δ::URA3 mph1Δ::KAN*
X4186-18B	*MATa RAD53-3Flag::LEU2 mec3Δ::URA3 smc6-P4-13myc::HIS3*
X4186-12C	*MATa RAD53-3Flag::LEU2 mec3Δ::URA3 smc6-P4-13myc::HIS3 mph1Δ::KAN*
X4187-6D	*MATa RAD53-3Flag::LEU2 rad24Δ::TRP1smc6-P4-13myc::HIS3 mph1Δ::KAN*
X3903-18D	*MATa trp1::TUB1-GFP::TRP1*
X3903-19C	*MATa trp1::TUB1-GFP::TRP1 smc6-P4-13myc::HIS3*
X3903-19D	*MATa trp1::TUB1-GFP::TRP1 smc6-P4-13myc::HIS3 TEL1-hy909::LEU2*

Strains in this study are derivatives of W1588-4C, a *RAD5* derivative of W303 (*MATa ade2-1 can1-100 ura3-1 his3-11,15 leu2-3112 trp1-1 rad5-535*). A single representative of each genotype is listed.

TABLE 1: Yeast strains used in this study.

Cell synchrony and MMS treatment

Cell synchronization was performed by adding α factor (Memorial Sloan-Kettering Cancer Center Proteomics Core) to cells growing in log phase to a final concentration of 5 μg/ml for ~2 h and evaluating the percentage of unbudded cells in the culture. Galactose induction was carried out as previously described (Bonilla *et al.*, 2008). In brief, cells were first arrested with α factor for 2 h, and then galactose was added for 2 h in the presence of α factor. The release from α factor was performed in the presence of MMS at a final concentration of 0.03 or 0.005% as indicated. Cell cycle progression was analyzed by FACS as performed previously (Zhao and Rothstein, 2002). One representative result is presented for each genotype.

Survival assays

Spot assays for detecting DNA damage sensitivity were carried out as described previously (Chen *et al.*, 2009). Briefly, log-phase cultures were serially diluted 10-fold and spotted onto agar plates containing yeast extract/peptone/dextrose media with the addition of the indicated doses of MMS. Plates were incubated at 30°C and photographed after at least 48 h. For killing curves, cultures challenged by MMS were taken at intervals, sonicated, and serially diluted before plating. An equal volume of 10% sodium thiosulfate was used to quench the effect of MMS in the sample before serial dilutions. The percentage of viable colonies was calculated by dividing the number of colonies by the number of cells plated based on the optical density readings of a spectrophotometer (Biomate 3;

Thermo Scientific, Waltham, MA). Because the plating efficiency of each genotype varies in normal growth conditions, the viability of each genotype in MMS at each time point was determined by normalizing the percentage of the viable colonies to its plating efficiency. Unpaired Student's *t* test was used for statistical analysis.

Two-dimensional gel electrophoresis and protein detection

The 2D gel electrophoresis was carried out and X-mols were quantified as described (Chen *et al*., 2009). To assay Rad53 phosphorylation and Sml1 protein levels, the trichloroacetic acid protein extraction method was used as originally described (Foiani *et al*., 1994). The extracts were separated on standard SDS–PAGE gels and Western blotted, followed by probing with anti-Flag (Sigma-Aldrich, St. Louis, MO) or anti-hemagglutinin (Memorial Sloan-Kettering Cancer Center Monoclonal Antibody Core Facility) antibodies to detect Rad53, anti-Sml1 antibody to detect Sml1, and YL1/2 antibody (AbD Serotec, Raleigh, NC) to detect tubulin. The abundance of a protein was quantified by measuring the intensity of its band using Image Gauge (Fujifilm, Tokyo, Japan). The percentage of Rad53 phosphorylation was calculated using the signal of Rad53-P divided by total Rad53 signal. At least two independent spore clones per genotype were examined for each genotype, and the representative results are shown.

PFGE and microscopy analysis

Chromosome plugs were prepared and PFGE was performed as previously described (Cremona *et al*., 2012). For microscopy, cells were fixed by addition of formaldehyde to a final concentration of 3.7% in the culture for 10 min, followed by washing with 0.1 M potassium phosphate, pH 8.1. Cells were then resuspended in a buffer of 1.2 M sorbitol and 0.1 M potassium phosphate, pH 8.1, and aliquots were stained with 4 μg/ml of Hoechst 33258 dye and processed for microscopy as previously described (Yong-Gonzales *et al*., 2012). The exposure times used for Tub1-GFP and Hoechst were 2 and 0.2 s respectively. All imaging was captured on an Axio Imager microscope (Carl Zeiss, Jena, Germany) with a 100× objective lens (numerical aperture 1.4). From 8 to 10 *Z*-sections with a 0.5-μm step size were taken to cover the whole yeast cell. Unpaired Student's *t* test was used for statistical analysis.

ACKNOWLEDGMENTS

We thank Maria Longhese (Università degli Studi di Milano-Bicocca, Milan, Italy) for the *TEL1-hy909* allele and David Toczyski (University of California at San Francisco, San Francisco, CA) for the strain containing the LacI-GFP fusions of Ddc1 and Ddc2; Koyi Choi for her help in generating some of the strains; and members of the Zhao lab for comments on the manuscript. This work was supported by National Institute of General Medical Science Grant R01 GM080670, American Cancer Society Research Scholar Grant RSG-12-013-01-CCG, and a Lymphoma Society Scholar Award to X.Z. and by Associazione Italiana per la Ricerca sul Cancro Grant IG 10637 and European Research Council Grant 242928 to D.B.

REFERENCES

Aguilera A, Gómez-González B (2008). Genome instability: a mechanistic view of its causes and consequences. Nat Rev Genet 9, 204–207.

Alabert C, Bianco JN, Pasero P (2009). Differential regulation of homologous recombination at DNA breaks and replication forks by the Mrc1 branch of the S-phase checkpoint. EMBO J 28, 1131–1141.

Baldo V, Testoni V, Lucchini G, Longhese MP (2008). Dominant *TEL1-hy* mutations compensate for Mec1 lack of functions in the DNA damage response. Mol Cell Biol 28, 358–375.

Ball LG, Zhang K, Cobb JA, Boone C, Xiao W (2009). The yeast Shu complex couples error-free post-replication repair to homologous recombination. Mol Microbiol 73, 89–102.

Barlow JH, Rothstein R (2009). Rad52 recruitment is DNA replication independent and regulated by Cdc28 and the Mec1 kinase. EMBO J 28, 1121–1130.

Bermudez-Lopez M, Ceschia A, de Piccoli G, Colomina N, Pasero P, Aragon L, Torres-Rosell J (2010). The Smc5/6 complex is required for dissolution of DNA-mediated sister chromatid linkages. Nucleic Acids Res 38, 6502–6512.

Bonilla CY, Melo JA, Toczyski DP (2008). Colocalization of sensors is sufficient to activate the DNA damage checkpoint in the absence of damage. Mol Cell 30, 267–276.

Branzei D, Foiani M (2010). Maintaining genome stability at the replication fork. Nat Rev Mol Cell Biol 11, 208–219.

Branzei D, Sollier J, Liberi G, Zhao X, Maeda D, Seki M, Enomoto T, Ohta K, Foiani M (2006). Ubc9- and Mms21-mediated sumoylation counteracts recombinogenic events at damaged replication forks. Cell 127, 509–522.

Cejka P, Bachrati CZ, Hickson ID, Kowalczykowski SC (2010). Rmi1 stimulates decatenation of double Holliday junctions during dissolution by Sgs1-Top3. Nat Struct Mol Biol 17, 1377–1382.

Cejka P, Kowalczykowski SC (2010). The full-length *Saccharomyces cerevisiae* Sgs1 protein is a vigorous DNA helicase that preferentially unwinds Holliday junctions. J Biol Chem 285, 8290–8301.

Chavez A, Agrawal V, Johnson FB (2010). Sumoylation and the structural maintenance of chromosomes (SMC) 5/6 complex slow senescence through recombination intermediate resolution. J Biol Chem 285, 11922–11930.

Chen Y-H, Choi K, Szakal B, Arenz J, Duan X, Ye H, Branzei D, Zhao X (2009). Interplay between the Smc5/6 complex and the Mph1 helicase in recombinational repair. Proc Natl Acad Sci USA 106, 21252–21257.

Choi K, Szakal B, Chen YH, Branzei D, Zhao X (2010). The Smc5/6 complex and Esc2 influence multiple replication-associated recombination processes in *Saccharomyces cerevisiae*. Mol Biol Cell 21, 2306–2314.

Cobb JA, Schleker T, Rojas V, Bjergbaek L, Tercero JA, Gasser SM (2005). Replisome instability, fork collapse, and gross chromosomal rearrangements arise synergistically from Mec1 kinase and RecQ helicase mutations. Genes Dev 19, 3055–3069.

Cremona CA, Sarangi P, Yang Y, Hang LE, Rahman S, Zhao X (2012). Extensive DNA damage-induced sumoylation contributes to replication and repair and acts in addition to the mec1 checkpoint. Mol Cell 45, 422–432.

Foiani M, Marini F, Gamba D, Lucchini G, Plevani P (1994). The B subunit of the DNA polymerase alpha-primase complex in *Saccharomyces cerevisiae* executes an essential function at the initial stage of DNA replication. Mol Cell Biol 14, 923–933.

Frei C, Gasser S (2000). The yeast Sgs1p helicase acts upstream of Rad53p in the DNA replication checkpoint and colocalizes with Rad53p in S-phase-specific foci. Genes Dev 14, 81–96.

Harvey SH, Sheedy DM, Cuddihy AR, O'Connell MJ (2004). Coordination of DNA damage responses via the Smc5/Smc6 complex. Mol Cell Biol 24, 662–674.

Hickson ID, Mankouri HW (2011). Processing of homologous recombination repair intermediates by the Sgs1-Top3-Rmi1 and Mus81-Mms4 complexes. Cell Cycle 10, 3078–3085.

Karras G, Fumasoni M, Sienski G, Vanoli F, Branzei D, Jentsch S (2013). Noncanonical role of the 9-1-1 clamp in the error-free DNA damage tolerance pathway. Mol Cell 49, 536–546.

Kegel A, Sjogren C (2010). The Smc5/6 complex: more than repair. Cold Spring Harb Symp Quant Biol 75, 179–187.

Lee SE, Pellicioli A, Vaze MB, Sugawara N, Malkova A, Foiani M, Haber JE (2003). Yeast Rad52 and Rad51 recombination proteins define a second pathway of DNA damage assessment in response to a single double-strand break. Mol Cell Biol 23, 8913–8923.

Li X, Heyer WD (2008). Homologous recombination in DNA repair and DNA damage tolerance. Cell Res 18, 99–113.

Liberi G *et al*. (2005). Rad51-dependent DNA structures accumulate at damaged replication forks in sgs1 mutants defective in the yeast ortholog of BLM RecQ helicase. Genes Dev 19, 339–350.

Lisby M, Barlow JH, Burgess RC, Rothstein R (2004). Choreography of the DNA damage response: spatiotemporal relationships among checkpoint and repair proteins. Cell 118, 699–713.

Mankouri HW, Ngo HP, Hickson ID (2007). Shu proteins promote the formation of homologous recombination intermediates that are processed by Sgs1-Rmi1-Top3. Mol Biol Cell 18, 4062–4073.

Mankouri HW, Ngo HP, Hickson ID (2009). Esc2 and Sgs1 act in functionally distinct branches of the homologous recombination repair pathway in *S. cerevisiae*. Mol Biol Cell 20, 1683–1694.
Petermann E, Orta ML, Issaeva N, Schultz N, Helleday T (2010). Hydroxyurea-stalled replication forks become progressively inactivated and require two different RAD51-mediated pathways for restart and repair. Mol Cell 37, 492–502.
Putnam CD, Jaehnig EJ, Kolodner RD (2009). Perspectives on the DNA damage and replication checkpoint responses in *Saccharomyces cerevisiae*. DNA Repair 8, 974–982.
Santocanale C, Diffley JF (1998). A Mec1- and Rad53-dependent checkpoint controls late-firing origins of DNA replication. Nature 395, 615–618.
Shirahige K, Hori Y, Shiraishi K, Yamashita M, Takahashi K, Obuse C, Tsurimoto T, Yoshikawa H (1998). Regulation of DNA-replication origins during cell-cycle progression. Nature 395, 618–621.
Shor E, Weinstein J, Rothstein R (2005). A genetic screen for *top3* suppressors in *Saccharomyces cerevisiae* identifies *SHU1*, *SHU2*, *PSY3* and *CSM2*: four genes involved in error-free DNA repair. Genetics 169, 1275–1289.
Sollier J, Driscoll R, Castellucci F, Foiani M, Jackson SP, Branzei D (2009). The *S. cerevisiae* Esc2 and Smc5-6 proteins promote sister chromatid junction mediated intra-S repair. Mol Biol Cell 20, 1671–1682.
Tanaka TU, Stark MJ, Tanaka K (2005). Kinetochore capture and bi-orientation on the mitotic spindle. Nat Rev Mol Cell Biol 6, 929–942.
Tercero JA, Longhese MP, Diffley JF (2003). A central role for DNA replication forks in checkpoint activation and response. Mol Cell 11, 1323–1336.
Thomas BJ, Rothstein R (1989). Elevated recombination rates in transcriptionally active DNA. Cell 56, 619–630.
Yeung M, Durocher D (2011). Srs2 enables checkpoint recovery by promoting disassembly of DNA damage foci from chromatin. DNA Repair 10, 1213–1222.
Yong-Gonzales V, Hang LE, Castellucci F, Branzei D, Zhao X (2012). The Smc5-Smc6 complex regulates recombination at centromeric regions and affects kinetochore protein sumoylation during normal growth. PloS One 7, e51540.
Zhao X, Blobel G (2005). A SUMO ligase is part of a nuclear multiprotein complex that affects DNA repair and chromosomal organization. Proc Natl Acad Sci USA 102, 4777–4782.
Zhao X, Chabes A, Domkin V, Thelander L, Rothstein R (2001). The ribonucleotide reductase inhibitor Sml1 is a new target of the Mec1/Rad53 kinase cascade during growth and in response to DNA damage. EMBO J 20, 3544–3553.
Zhao X, Muller EG, Rothstein R (1998). A suppressor of two essential checkpoint genes identifies a novel protein that negatively affects dNTP pools. Mol Cell 2, 329–340.
Zhao X, Rothstein R (2002). The Dun1 checkpoint kinase phosphorylates and regulates the ribonucleotide reductase inhibitor Sml1. Proc Natl Acad Sci USA 99, 3746–3751.